# Modeling the Effects of Initial Spacing on Stand Basal Area Development of Loblolly Pine

**Clara Antón-Fernández, Harold E. Burkhart, and Ralph L. Amateis**

**Abstract:** Several studies have reported that in loblolly pine stands with high initial density, basal area declines after reaching maximum carrying capacity. This behavior is not reproduced by most basal area development models because the functions used are sigmoid and nondecreasing, tending toward an asymptote. We used a combined exponential and power function to model the impact of initial density on the basal area development of loblolly pine in a spacing trial. The combined exponential and power function is sufficiently flexible to describe both the asymptotic behavior of the wider initial spacing plots and the decrease in basal area after culmination of the closer spacings. We modified the original function to account for the time lag between stand establishment (age = 0) and basal area establishment (age > 0), by allowing the origin of the function to be different than age = 0. Two final models are presented: a model fitted using the population-average (PA) approach and a model fitted using the mixed-effects (ME) approach. At the fixed-effects level, the PA and ME models are not equivalent, and, therefore, the appropriate model should be selected according to the availability of previous data and the objectives of the prediction. If previous observations are available, they can be used to improve the predictions using the ME model. FOR. SCI. 58(2):95–105.

**Keywords:** growth, yield, initial density, stand dynamics, *Pinus taeda*

STAND BASAL AREA development is a key component for stand growth modeling (von Gadow and Hui 1999). Both before and after the onset of intraspecific competition, stand basal area (BA) is greatly influenced by the initial number of trees planted. Initial density, together with survival rates and site quality, determines the growing space available for individual trees and, thus, the age at which intraspecific competition begins. The earlier the intraspecific competition begins, the earlier the effects of competition on diameter growth and mortality will start. The equilibrium between diameter growth and mortality, both largely influenced by the initial density of the stand, dictates the dynamics of BA.

Many model forms have been used to describe stand BA development for even-aged stands. Most model forms are sigmoid and nondecreasing (e.g., Burkhart and Sprinz 1984, Radtke and Burkhart 1999). Although these types of functions might perform well in average stand densities, they are not flexible enough to characterize the range of behaviors that have been observed in loblolly pine BA development, particularly at close spacings (spacing is defined as the growing space, area, available per tree). When the effect of initial spacing in loblolly pine BA development is studied, some researchers have found that stand BA in close initial spacings (generally, less than 4 $m^2$/tree) decreases after reaching its maximum. For example, Buford (1991) observed a decline in BA after age 20 for the 1.8 × 1.8-m spacing in data from a loblolly pine spacing study. Matney and Sullivan (1982) also reported a decline in BA starting at approximately ages 15–20 for high-density unthinned plots of loblolly pine. This behavior of BA in close initial spacing is reproduced by several loblolly pine growth and yield models (Buford 1991). In models that show a turndown in BA, BA is usually derived from diameter growth, often driven by dominant height growth, and mortality and not modeled directly. For example, the model of Bailey et al. (1985), which calculates BA as a function of quadratic mean diameter and number of trees, shows decreasing BA after reaching a maximum for high initial stand densities. Models that directly predict BA development are usually nondecreasing and, thus, unable to model the behavior of stands planted at close spacing. In an attempt to overcome this problem Harrison and Daniels (1988) used a correction factor to modify the asymptotic nondecreasing form of their BA model. Because the correction factor was a function of relative spacing, Harrison and Daniels's model required an estimate of dominant height and survival to model the decline in BA.

The objective of the research reported here was to model BA production directly for varying initial planting densities. Data from annual measurements of a loblolly pine spacing trial over a 25-year span provided an empirical base for modeling the effects of planting density on BA development. To accommodate different prediction objectives and situations with varying amounts of previous measurement data, both population-average and mixed-effects approaches were applied for modeling stand BA development.

Manuscript received June 14, 2010; accepted February 8, 2011; published online February 2, 2012; http://dx.doi.org/10.5849/forsci.10-074.

Clara Antón Fernández, this work was completed at Virginia Tech; current address, Norwegian Forest and Landscape Institute, Postboks 115, Ås, 1431, Norway—Phone: 94158990; caf@skogoglandskap.no. Harold E. Burkhart, Virginia Tech—burkhart@vt.edu. Ralph L. Amateis, Virginia Tech—ralph@vt.edu.

Acknowledgments: Support from the Forest Modeling Research Cooperative at Virginia Tech for field plot establishment, maintenance, and financial support for data analysis is gratefully acknowledged. This work was completed when C. Antón-Fernández was a Postdoctoral Research Associate at Virginia Tech.

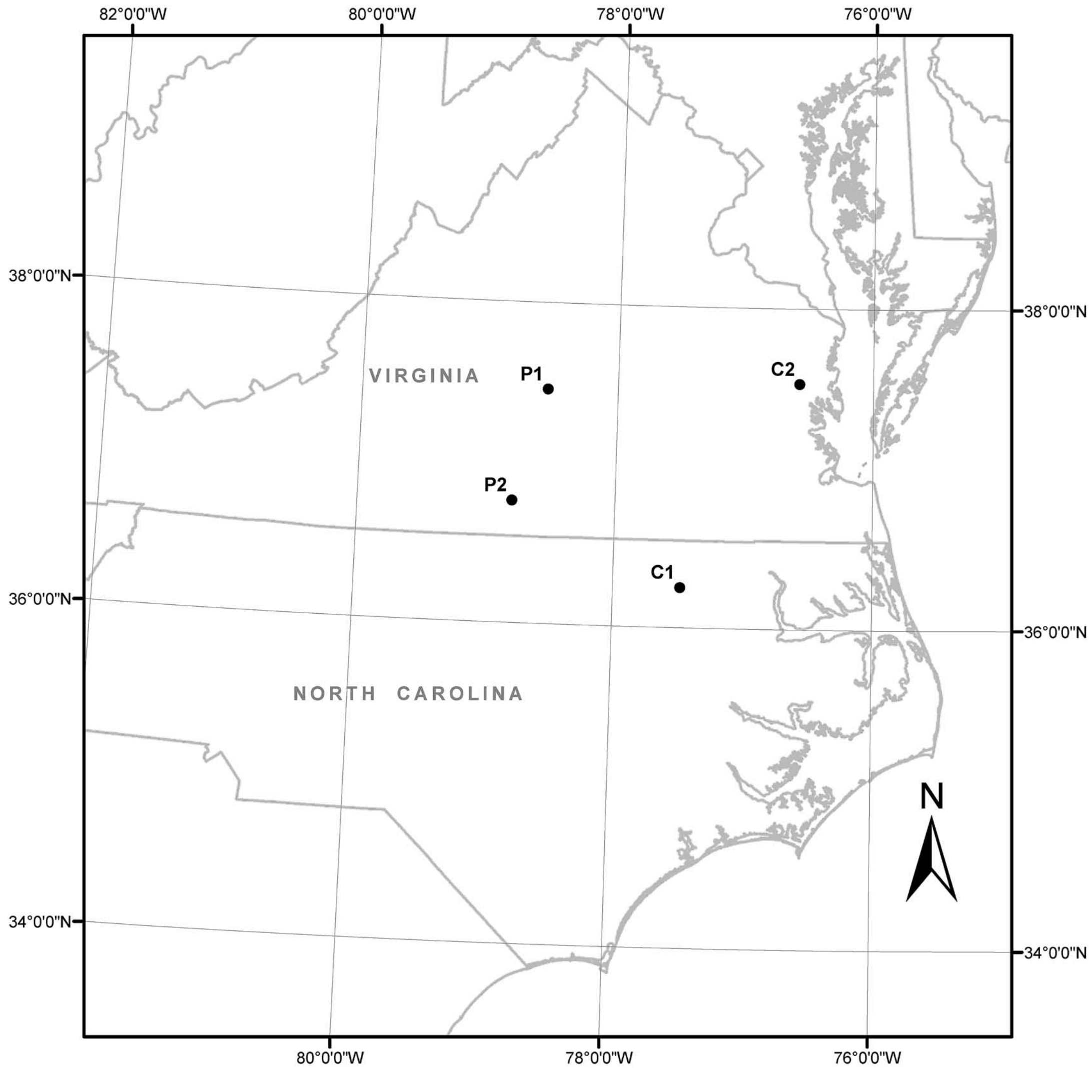


**Figure 1. Geographical location of the spacing trial replicates (three replicates at each of the four locations: P1 and P2 are Piedmont sites; C1 and C2 are coastal plain sites).**

## Background on Subject-Specific and Population-Average Approaches

Data collected for forest growth and yield modeling are typically grouped. For example, if we use in our analysis measurements taken from two contiguous plots, the data collected cannot be considered independent. This lack of independence hinders the possibility of using traditional techniques such as nonlinear least squares. To overcome this problem two main approaches have been developed: subject-specific (SS), and population-average (PA) (Zeger et al. 1988). Models of the SS type represent the covariance structure induced by the grouping of the data by allowing some of the parameters that define the model to vary with group (e.g., stand) through the incorporation of random effects. An example of a SS approach is mixed-effects (ME) models, in which the SS effects are assumed to follow a parametric distribution. PA models directly model the within-group error covariance structure, without explicitly accounting for subject-to-subject heterogeneity.

Typically, BA is modeled with a nonlinear function of several covariates, which could include variables such as age (A), site index (SI), initial spacing (S), or thinning treatment, that is,

$$\mathbf{BA}_i = f(\mathbf{X}_i, \boldsymbol{\beta}) + \boldsymbol{\varepsilon}_i,$$

where $\mathbf{BA}_i$ is a vector of BA measurements for stand $i$, $\mathbf{X}_i$ is a matrix of covariates, $\boldsymbol{\beta}$ is a vector of fixed-effects parameters, and $\boldsymbol{\varepsilon}_i$ is a vector of error terms. The PA approach focuses on modeling the mean, or expectation, of BA,

$$\mathrm{E}(\mathbf{BA}_i) = f(\mathbf{X}_i, \boldsymbol{\beta}).$$

Thus, the parameters of a PA model are population-average responses to the covariates. A ME model focuses, on the other hand, on the individual response, modeling BA as a function of a vector of fixed-effects parameters ($\boldsymbol{\beta}$) common to all subjects and a vector of random effects ($\mathbf{u}_i$) unique for subject $i$, which is assumed to follow a multivariate normal distribution with mean zero and a variance-covariance matrix pounds per square inch. That is,

$$\mathbf{BA}_i = f(\mathbf{X}_i, \boldsymbol{\beta}, \mathbf{u}_i) + \boldsymbol{\varepsilon}_i.$$

The fixed-effects parameters of a ME model should be interpreted as the typical response of an individual and not as the population-average response.

When a parameter estimation approach is selected, the objectives of the analysis should be taken into account. If the focus is exclusively on making inferences about model parameters, then the PA approach is adequate when the interest lies on the PA response to changing covariates; the SS approach is preferred when the focus is on the typical response of an individual to changing covariates (Davidian and Giltinan 1995, Diggle et al. 2002). If the focus is on prediction, then the PA approach has a smaller prediction error than the SS approach when the SS response is computed using only the fixed-effects parameters of the ME models. If previous measurements are available to estimate the random effects of the SS model, then the SS predictions are more accurate than the PA predictions (Meng et al. 2009).

Both PA and SS (ME) approaches were used in this study to model the development of stand BA across a wide range of initial planting densities. Data from a loblolly pine spacing trial were used in these analyses.

# Data

Data used for this study were from a spacing study maintained by the Forest Modeling Research Cooperative at Virginia Polytechnic Institute and State University (Virginia Tech). Four locations were included in this spacing study, two in the Piedmont area (P1 and P2 in Figure 1) and two in the coastal plain region (C1 and C2 in Figure 1). At each location three replicates (blocks) were planted, and, in each replicate, 16 plots with a different tree arrangement in each were established. A representative block is illustrated in Figure 2. Although each of the 16 plots has a different tree arrangement, some of them have the same spacing (Table 1). There were a total of nine different initial spacings. The diameter of each tree was measured every year from age 1 to age 25. The diameter for each tree in the study was measured at ground level from age 1 through 5 and at breast height from age 5 through age 25. Total height of each tree was measured each year from age 1 through age 10 and every 2 years thereafter.

During the 25 years of the study several events affected the integrity of some of the plots. At age 11, several plots of

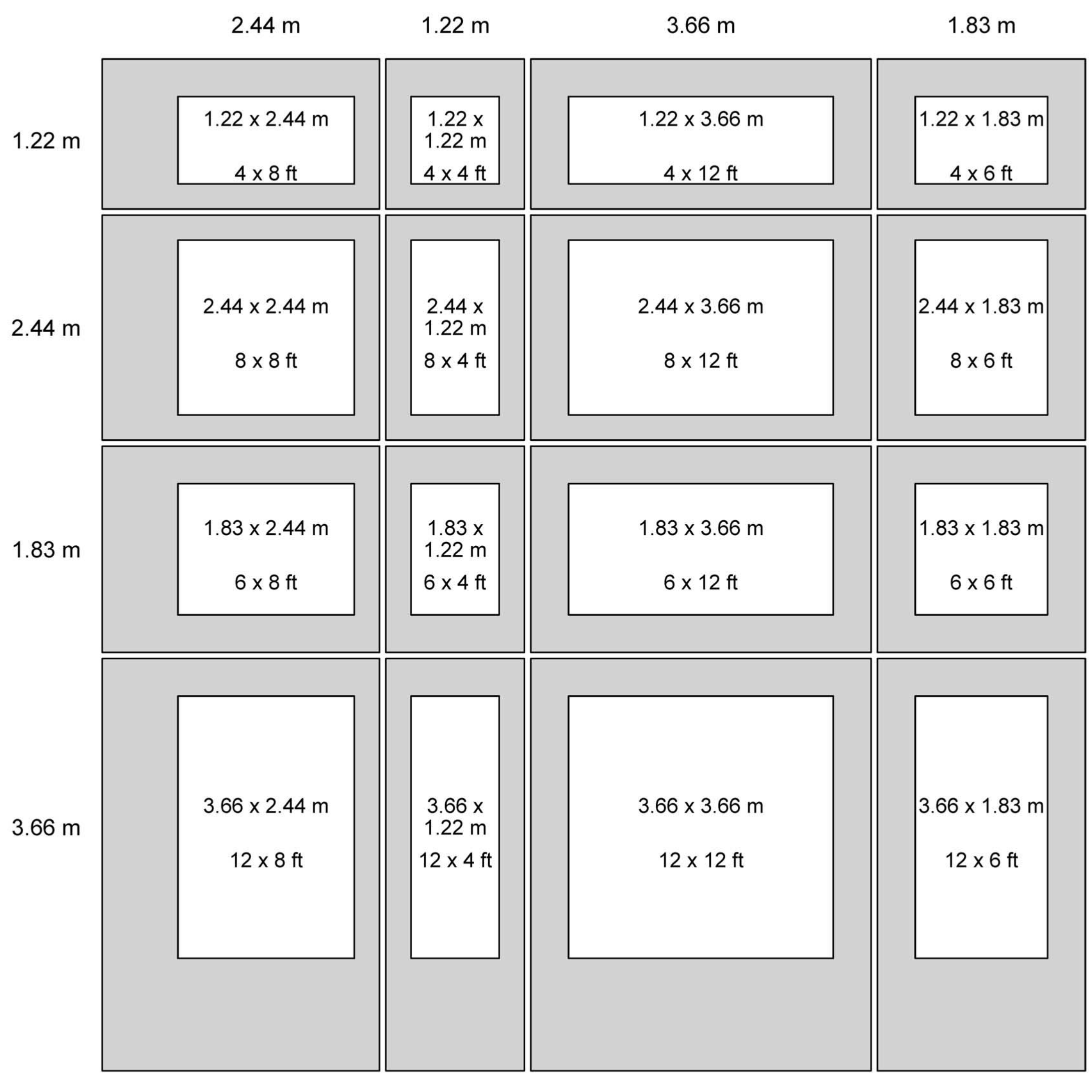


**Figure 2. A representative block on the spacing trial design. The gray areas indicate the border zones.**

Table 1. **Summary of the fitting data set.**

| Spacing ($m^2$/tree) | Tree arrangements (m) | Trees/ha | No. plots | Mean values at age 25[a] | |
|---|---|---|---|---|---|
| | | | | dbh | DH |
| 1.49 | 1.22 × 1.22 | 6,730 | 12 | 17.0 | 19.0 |
| 2.23 | 1.22 × 1.83; 1.83 × 1.22 | 4,485 | 24 | 16.9 | 19.6 |
| 2.97 | 1.22 × 2.44; 2.44 × 1.22 | 3,365 | 24 | 18.7 | 20.1 |
| 3.34 | 1.83 × 1.83 | 2,990 | 12 | 18.8 | 19.9 |
| 4.46 | 1.22 × 3.66, 3.66 × 1.22; 1.83 × 2.44, 2.44 × 1.83 | 2,240 | 48 | 20.7 | 20.8 |
| 5.95 | 2.44 × 2.44 | 1,680 | 12 | 21.7 | 21.4 |
| 6.69 | 1.83 × 3.66; 3.66 × 1.83 | 1,495 | 24 | 22.8 | 21.1 |
| 8.92 | 2.44 × 3.66; 2.44 × 3.6 | 1,120 | 24 | 24.4 | 21.5 |
| 13.38 | 3.66 × 3.66 | 747 | 12 | 28.0 | 22.0 |

The initial number of trees planted per plot is 49 for all spacings. dbh, mean diameter at breast height (cm) for a given initial spacing; DH, mean height (m) of undamaged trees with diameter greater than the quadratic mean diameter (m).
[a] Summary data for age 25 are averages over all locations and replicates.

blocks 2 and 3 at location P1 suffered severe ice damage (Amateis and Burkhart 1996). Data from this location for ages 12 and older for seven plots at block 2 and nine plots at block 3 were not considered for any of the analyses in this study. At age 18, all plots from location P2 were dropped from the study because of thinning in the adjacent stand. At age 19 Hurricane Isabella damaged one plot at block 2 in C2. Data for that plot after age 19 were not used. At age 20 southern pine beetle (*Dendroctonus frontalis* Zimm.) severely affected two blocks at P1. Data for ages 21 and older at these blocks of P1 were not used.

We considered spacing as the initial growing space (area) available per tree, independently of the rectangularity (Table 1). The design of the study was intended to examine the effect of spacing and rectangularity on development of loblolly pine stands and, thus, the degree of rectangularity varied among plots. Because the effect of rectangularity in this spacing trial has proven to be negligible for the main tree variables, including diameter (Sharma et al. 2002a,b), we modeled spacing effects based on the average space available per tree regardless of the configuration of that space.

## Methodology

### *Model Form*

A preliminary graphical analysis of the data revealed a tendency of the plots with closer initial spacings to reach a maximum BA and then decrease (Figure 3). Plots with wider initial spacing tended to increase asymptotically, at least until age 25. Hence, the model should allow for both behaviors, the decrease after reaching a maximum at the closer initial spacings and the asymptotic behavior of the wider initial spacings.

For this study, we sought a model form that was flexible enough to describe both the asymptotic behavior of the wider initial spacing plots and the decrease in BA after culmination of the closer spacings. The type II combined exponential and power function (1) (Sit and Poulin-Costello 1994) provided this flexibility. The type II combined exponential and power function has the form

$$Y = \alpha X^{\beta} e^{\theta X}, \quad (1)$$

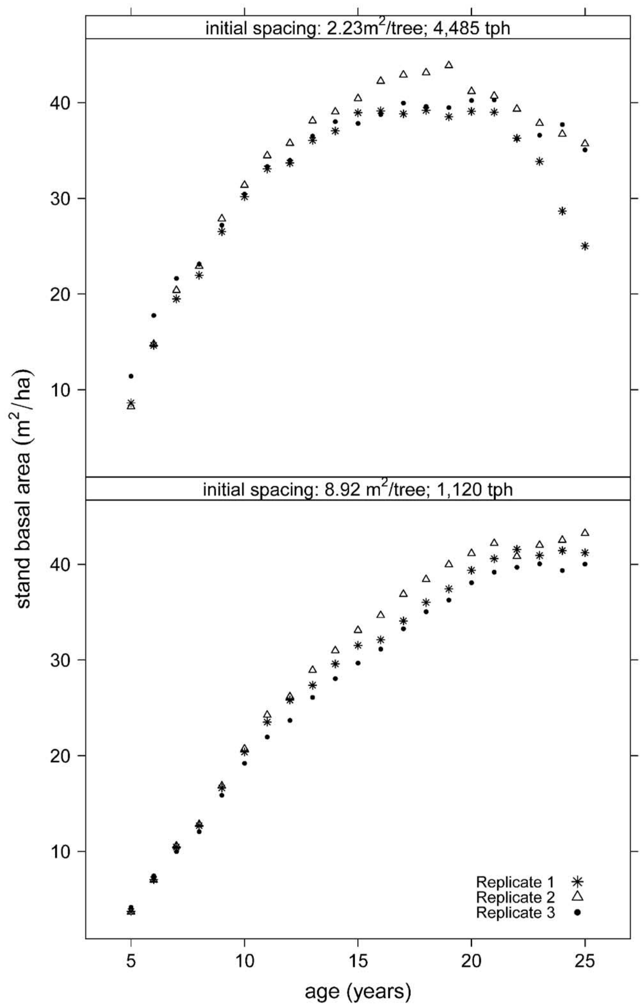


Figure 3. **An example of differences in the BA development pattern in close and wide spacings. tph, trees per hectare.**

where $Y$ is the independent variable, $X$ is the dependent variable, and $\alpha$, $\beta$, and $\theta$ are parameters.

This equation passes, by definition, through the origin ($Y = 0$, $X = 0$). In terms of BA, that would force the development of BA to start at age 0 (BA = 0, age = 0). However, because we define BA as the cross-sectional area *at breast height,* the stand BA is not defined until the stand reaches breast height. Thus, the origin of the model should be allowed to differ from zero ($Y = 0$, $X > 0$). Hence, we added a new parameter, $\omega$, which accounts for the time between stand establishment and stand BA establishment. The final model form (2) has four parameters ($\alpha$, $\beta$, $\theta$, and $\omega$):

$$Y = \alpha(A - \omega)^{\beta} e^{\theta(A-\omega)} \quad \text{Defined for} \quad A \geq \omega. \quad (2)$$

We initially explored the pattern of the model parameters with respect to initial spacing by allowing the parameters of model 2 to freely change with initial spacing. For this exploratory step we used nonlinear least squares, and we ignored heteroscedasticity and autocorrelation in the errors. To improve convergence during the fitting of the ME model, parameter $\beta$ was kept constant for all spacings. This constraint facilitated the convergence of the model and resulted in an adequate fit to the data during the fitting of the final models. Graphical analysis of the variation of the parameters (Figure 4) with spacing ($S$) showed that $\alpha$ and $\theta$ sharply changed at close initial spacings and tended to reach an asymptote at wider initial spacings, whereas $\omega$ increased proportionally to initial spacing. This suggested including a combination of $S$ and $S^{-1}$ or $S$ and $\log(S)$, for representing parameters $\alpha$ and $\theta$ and $S$ for modeling parameter $\omega$. The $S$ and $S^{-1}$ combination for $\alpha$ and $\theta$ produced the best results as measured by the log-likelihood, the Akaike information criterion (Akaike 1974), and the Bayesian information criterion (Schwarz 1978). Including the corresponding $S$ variables, the basic form of the model is

$$BA = (\alpha_0 + \alpha_1 S + \alpha_2 S^{-1}) \times (A - \omega)^{\beta_0} e^{(\theta_0 + \theta_1 S + \theta_2 S^{-1})(A-\omega)} \quad \text{Defined for } A \geq \omega.$$
$$\omega = \omega_0 + \omega_1 S \quad (3)$$

We fitted two models to this basic form of the model, a ME model and a PA model. Both models were fitted using the nlme package (Pinheiro et al. 2009) in R (R Development Core Team 2009).

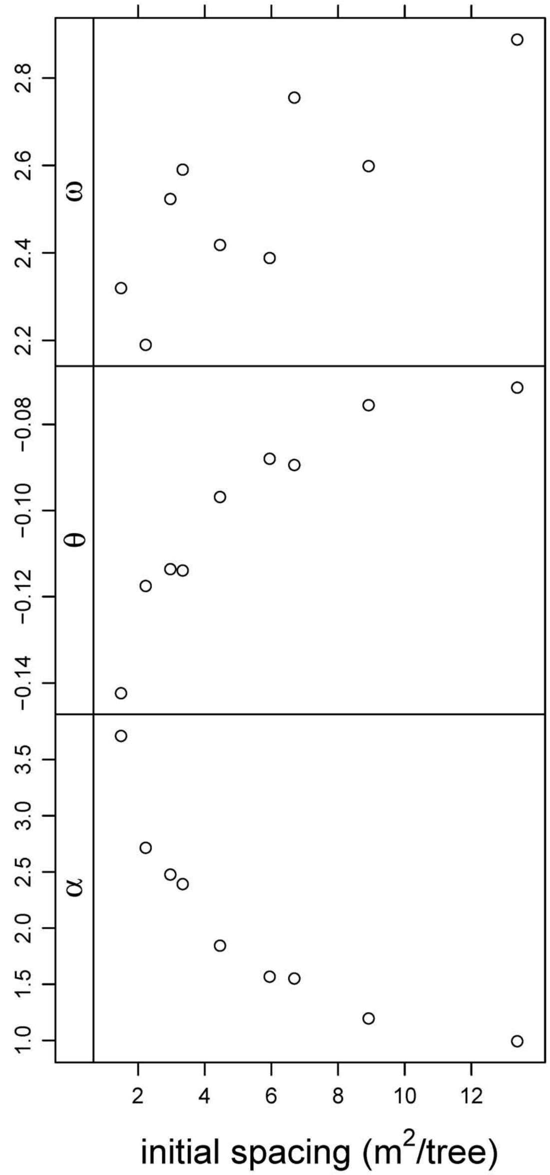


**Figure 4. Parameter estimates of model 2 when fitted separately for each spacing.**

## *Model Fitting*

### *ME model*

Following Pinheiro and Bates (2000), a general single-level nonlinear ME model (nlme) for modeling stand BA with consecutive measurements taken at each stand (single level of grouping) can be defined as

$$y_{ij} = f(\boldsymbol{\phi}_{ij}, \boldsymbol{\nu}_{ij}) + \varepsilon_{ij}, \quad i = 1, \ldots, M, \quad j = 1, \ldots, n_i, \quad (4)$$

where $y_{ij}$ is the $j$th observation of stand BA from the $i$th stand, $M$ is the number of stands, $n_i$ is the number of observations on the $i$th stand, $f$ is a general, real-valued, differentiable nonlinear function of a stand-specific parameter vector $\boldsymbol{\phi}_{ij}$ and a covariate vector $\boldsymbol{\nu}_{ij}$, and $\boldsymbol{\varepsilon}_{ij}$ is the normally distributed within-group error term. The stand-specific parameter vector $\phi_{ij}$ is modeled as

$$\boldsymbol{\phi}_{ij} = \mathbf{A}_{ij}\boldsymbol{\beta} + \mathbf{B}_{ij}\mathbf{b}_i, \quad \mathbf{b}_i \sim \mathrm{N}(\mathbf{0}, \boldsymbol{\Psi}) \quad (5)$$

where $\boldsymbol{\beta}$ is a $p$-dimensional vector of fixed-effects, $\mathbf{b}_i$ is a $q$-dimensional random-effects vector associated with the $i$th group (not varying with $j$) with variance-covariance matrix $\boldsymbol{\Psi}$, $p$ is the number of fixed-effects parameters in the model, $q$ is the number of random-effects parameters in the model, and the design matrices $\mathbf{A}_{ij}$, and $\mathbf{B}_{ij}$ are of size $r \times p$ and $r \times q$, respectively.

We can write Equations 4 and 5 in matrix form as

$$\mathbf{y}_i = \mathbf{f}_i(\boldsymbol{\phi}_i, \boldsymbol{\nu}_i) + \boldsymbol{\varepsilon}_i$$
$$\boldsymbol{\phi}_i = \mathbf{A}_i\boldsymbol{\beta} + \mathbf{B}_i\mathbf{b}_i \quad (6)$$

It is assumed that observations corresponding to different groups (stands) are independent and that the within-group errors $\boldsymbol{\varepsilon}_i$ are independently distributed as $\mathrm{N}(\mathbf{0}, \sigma^2\mathbf{I})$ and independent of the $\mathbf{b}_i$. This assumption is relaxed for the extended nlme models (see next section).

Several methods have been developed to estimate the parameters of nlme models. The parameters can be estimated either by maximum likelihood or by restricted maximum likelihood based on the marginal density of the responses $\mathbf{y}$:

$$p(\mathbf{y}|\boldsymbol{\beta}, \sigma^2, \boldsymbol{\Psi}) = \int p(\mathbf{y}|\mathbf{b}, \boldsymbol{\beta}, \sigma^2) p(\mathbf{b}|\boldsymbol{\Psi})\, d\mathbf{b}, \quad (7)$$

where $p(\mathbf{y}|\boldsymbol{\beta}, \sigma^2, \boldsymbol{\Psi})$ is the marginal density of $\mathbf{y}$, $p(\mathbf{y}|\mathbf{b}, \boldsymbol{\beta}, \sigma^2)$ is the conditional density of $\mathbf{y}$ given the random effects $\mathbf{b}$, and $p(\mathbf{b}|\boldsymbol{\Psi})$ is the marginal distribution of $\mathbf{b}$.

Maximization of Equation 7 requires solution of the integral over the random effects. Because the function $f$ is usually nonlinear in the random effects, the integral in Equation 7 generally does not have a closed-form expression. Lindstrom and Bates (1990) proposed a method to approximate the likelihood function in Equation 7 that alternates between two steps, a penalized nonlinear least-squares step and a linear mixed-effects step. This method is the one implemented in the nlme package (Pinheiro et al. 2009) in R (R Development Core Team 2009). Details about the algorithm can be found in Chapter 7 of Pinheiro and Bates (2000).

### *Extended ME*

When the within-group errors are correlated and/or heteroscedastic, the nlme model can be extended to allow for heteroscedastic and correlated errors. That is, $\boldsymbol{\varepsilon}_i \sim N(\mathbf{0}, \sigma^2\boldsymbol{\Lambda}_i)$, where the variance–covariance structure $\boldsymbol{\Lambda}_i$, parametrized by a fixed set of parameters $\boldsymbol{\lambda}$, can be decomposed as

$$\boldsymbol{\Lambda}_i = \mathbf{V}_i \mathbf{C}_i \mathbf{V}_i,$$

where $\mathbf{V}_i$ is a positive definite diagonal matrix, that is, with all diagonal elements equal to 1, and describes the variance of the within-group errors and $\mathbf{C}_i$ is a correlation matrix that describes the correlation of the within-group errors. That is,

$$\mathrm{Var}(\varepsilon_{ij}) = \sigma^2[\mathbf{V}_i]_{jj} \quad \mathrm{cor}(\varepsilon_{ij}, \varepsilon_{ij'}) = [\mathbf{C}_i]_{jj'}.$$

The log-likelihood corresponding to the extended nlme model corresponds to a basic nlme model (Pinheiro and Bates 2000). Hence, similar algorithms and approximations to the basic nlme are applied to the extended nlme. Both the basic nlme and the extended nlme described above are easily extrapolated to the case of multiple-level models (see Chapter 7 in Pinheiro and Bates 2000).

### *PA model*

The PA model can be considered a simplification of the extended nlme model, where the within-group variance-covariance structure is represented by $\boldsymbol{\Lambda}_i$, but there are no random effects to account for within-group dependence:

$$y_{ij} = f(\boldsymbol{\phi}_{ij}, \boldsymbol{\nu}_{ij}) + \varepsilon_{ij}, \quad i = 1, \ldots, M, \quad j = 1, \ldots, n_i$$
$$\boldsymbol{\phi}_{ij} = \mathbf{A}_{ij}\boldsymbol{\beta}, \quad (8)$$

where all the terms are defined as in the nlme model. We can write Equation 8 in matrix form as

$$\mathbf{y}_i = \mathbf{f}_i(\boldsymbol{\phi}_i, \boldsymbol{\nu}_i) + \varepsilon_i$$
$$\boldsymbol{\phi}_i = \mathbf{A}_i\boldsymbol{\beta}, \quad \varepsilon_i \sim N(\mathbf{0}, \sigma^2\boldsymbol{\Lambda}_i). \quad (9)$$

Because $\boldsymbol{\Lambda}_i$ is positive-definite, it admits an invertible square root $\boldsymbol{\Lambda}_i^{1/2}$, with inverse $\boldsymbol{\Lambda}_i^{-1/2}$ such that $\boldsymbol{\Lambda}_i = \boldsymbol{\Lambda}_i^{T/2}\boldsymbol{\Lambda}_i^{1/2}$. Then, if we define $\mathbf{y}_i^*$ as

$$\mathbf{y}_i^* = \boldsymbol{\Lambda}_i^{-T/2}\mathbf{y}_i$$
$$\mathbf{f}_i^*(\boldsymbol{\phi}_i, \boldsymbol{\nu}_i) = \boldsymbol{\Lambda}_i^{-T/2}\mathbf{f}_i(\boldsymbol{\phi}_i, \boldsymbol{\nu}_i)$$
$$\boldsymbol{\varepsilon}_i^* = \boldsymbol{\Lambda}_i^{-T/2}\boldsymbol{\varepsilon}_i$$

Equation 9 can be reexpressed as a classic nonlinear regression model:

$$\mathbf{y}_i^* = \mathbf{f}_i^*(\boldsymbol{\phi}_i, \boldsymbol{\nu}_i) + \boldsymbol{\varepsilon}_i^*$$
$$\boldsymbol{\phi}_i = \mathbf{A}_i\boldsymbol{\beta}, \quad \varepsilon_i^* \sim N(\mathbf{0}, \sigma^2\mathbf{I}) \quad (10)$$

Several methods to estimate the parameters in 10 exist. There are full-likelihood and nonlikelihood approaches. Among the latter, the most popular is the generalized estimating equation (Zeger et al. 1988), which treats the correlation structure as a nuisance, and it is not an adequate approach when the correlation structure is of interest. We focus on the full-likelihood approach, which is the one implemented in the nlme package in R.

The log-likelihood function for model 10 is

$$l(\boldsymbol{\beta}, \sigma^2, \boldsymbol{\Delta}|\mathbf{y}) = -\frac{1}{2}\left\{N\log(2\pi\sigma^2) + \sum_{i=1}^{M}\left[\frac{\|\mathbf{y}_i^* - \mathbf{f}_i^*(\boldsymbol{\beta})\|}{\sigma^2} + \log|\boldsymbol{\Lambda}_i|\right]\right\},$$

where $\mathbf{f}_i^*(\boldsymbol{\beta}) = \mathbf{f}_i^*(\boldsymbol{\phi}_i, \boldsymbol{\nu}_i)$ and $M$ is the total number of observations.

The maximum likelihood estimator of $\sigma^2$ for fixed $\boldsymbol{\beta}$ and $\boldsymbol{\lambda}$, that is $\hat{\sigma}^2(\boldsymbol{\beta}, \lambda)$, is used to obtain the profiled log-likelihood $l(\boldsymbol{\beta}, \boldsymbol{\lambda}|\boldsymbol{y})$, which is used to obtain the maximum likelihood estimates of $\boldsymbol{\beta}$ and $\boldsymbol{\lambda}$. Given the current estimate $\hat{\boldsymbol{\lambda}}^{(w)}$ of $\boldsymbol{\lambda}$, a new estimate $\hat{\boldsymbol{\beta}}^{(w)}$ for $\boldsymbol{\beta}$ is produced by maximizing $l(\boldsymbol{\beta}, \hat{\boldsymbol{\lambda}}^{(w)})$. The roles are then reversed, and a new estimate $\hat{\boldsymbol{\lambda}}^{(w+1)}$ is produced by maximizing $l(\hat{\boldsymbol{\beta}}^{(w)}, \boldsymbol{\lambda})$. The procedure iterates between the two optimizations until convergence is met. For a comparison of PA models versus SS models in a forestry context, see Meng et al. (2009).

### *Significance tests and diagnostics for assessing the quality of the fit*

Models were compared using likelihood ratio tests (LRTs) when nested and the Akaike information criterion and Bayesian information criterion, otherwise. The significance of the fixed-effects parameters for both the ME and PA models was assessed with conditional $t$ tests and $F$ tests (Pinheiro and Bates 2000). Assumptions about the within-group errors and random effects were assessed graphically

Table 2. Estimates and lower and upper confidence limits of the parameters for the ME approach model 11.

| | Estimate | Lower | Upper |
|---|---|---|---|
| $\alpha_0$ | 2.24126 | 1.89786 | 2.58465 |
| $\alpha_1$ | −0.06315 | −0.08507 | −0.04123 |
| $\alpha_2$ | 5.51533 | 4.39390 | 6.63677 |
| $\hat{\psi}_{2,11}$ | 1.19427 | 0.67963 | 2.09864 |
| $\hat{\psi}_{3,11}$ | 1.04038 | 0.68724 | 1.57497 |
| $\omega_0$ | 2.67811 | 2.07919 | 3.27703 |
| $\omega_1$ | 0.08647 | 0.07068 | 0.10226 |
| $\hat{\psi}_1$ | 0.58246 | 0.27967 | 1.21308 |
| $\hat{\psi}_{2,22}$ | 0.21974 | 0.12541 | 0.38502 |
| $\beta$ | 1.35881 | 1.31477 | 1.40285 |
| $\theta_0$ | −0.06335 | −0.07047 | −0.05624 |
| $\theta_1$ | 0.00130 | 0.00077 | 0.00183 |
| $\theta_2$ | −0.07497 | −0.09379 | −0.05615 |
| $\hat{\psi}_{2,33}$ | 0.01704 | 0.01009 | 0.02879 |
| $\hat{\psi}_{3,22}$ | 0.01901 | 0.01250 | 0.02891 |
| $\hat{\psi}_{3,12}$, $\hat{\psi}_{3,21}$ | −0.81472 | −0.91641 | −0.61422 |
| $\kappa$ | 0.88259 | 0.84514 | 0.91142 |
| $\delta_{1,P1}$ | 0.28061 | 0.36465 | 0.44869 |
| $\delta_{1,P2}$ | 0.24912 | 0.34330 | 0.43749 |
| $\delta_{1,C1}$ | 0.46560 | 0.53191 | 0.59821 |
| $\delta_{1,C2}$ | 0.49560 | 0.56304 | 0.63049 |
| $\delta_{2,P1}$ | −0.57121 | −0.48405 | −0.39689 |
| $\delta_{2,P2}$ | −0.39371 | −0.28667 | −0.17962 |
| $\delta_{2,C1}$ | −0.69346 | −0.61628 | −0.53910 |
| $\delta_{2,C2}$ | −0.64183 | −0.56781 | −0.49379 |

All parameters were statistically significant at $\alpha = 0.001$.

and analytically using LRTs and numerical summaries including intervals of the estimated parameters. The model-building strategy for the ME model conforms, in general, to the procedure described in detail by Zhao et al. (2005).

Similar graphical tools were used to check the degree to which different assumptions were met in the ME and PA models. We assessed the need and adequacy of autocorrelation functions using plots of the empirical autocorrelation function of the normalized residuals. To assess the assumption of constant variance of the within-group errors, plots of the residuals versus the fitted responses from the model were used. The assumption of normality for the within-group errors was assessed with normal probability plots of the residuals. For the ME model, assumptions on the random effects were assessed using several diagnostic plots. Normal probability plots of the estimated random effects were used to check marginal normality. Scatter plot matrices of the estimated random effects were used to check the structure of the random-effects covariance matrix.

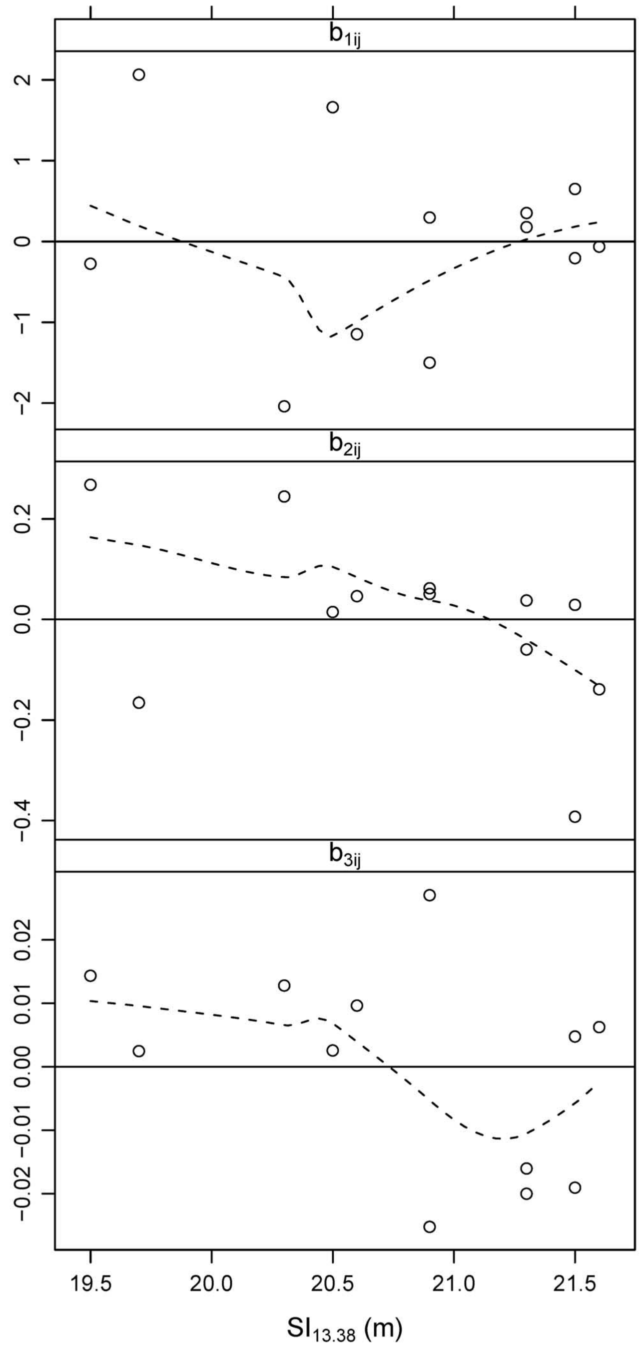


Figure 5. Pattern of the estimated random effects at the replicate level with respect to $SI_{13.38}$ (average height of trees with dbh larger than the quadratic mean diameter at age 25 in the widest spacing [13.38 $m^2$/tree]). A loess (local regression) smoothing line is shown with a dashed pattern.

# Results

## *ME Model*

The final ME model is defined in 11, and parameters, including lower and upper confidence limits, are shown in Table 2. Random parameters were found to be significant, according to LRTs, at the location level in the intercept of $w$ ($b_{2i}$), at the replicate level in $S^{-1}$ of $\alpha$ ($b_{1ij}$) and $\theta$ ($b_{3ij}$) and in the intercept of $w$ ($b_{2ij}$), and at the plot level in $S^{-1}$ of $\alpha$ ($b_{1ijk}$) and $\theta$ ($b_{3ijk}$). Scatterplot matrices of the estimated random effects showed correlation between the random effects at the plot level for $S^{-1}$ in $\alpha$ and $\theta$, and LRTs confirmed the need to model the covariance between these two terms. All parameters were significant at $\alpha = 0.001$. Model 11 follows:

$$BA_{ijkl} = (\alpha_0 + \alpha_1 S + (\alpha_2 + b_{1ij} + b_{1ijk})S^{-1}) \times (A - \omega)^{\beta_0} e^{(\theta_0 + \theta_1 S + (\theta_2 + b_{3ij} + b_{3ijk})S^{-1})(A-\omega)} + \varepsilon_{ijkl}$$

$$\omega = \omega_0 + b_{2i} + b_{2ij} + \omega_1 S \quad \text{Defined for} \quad A \geq \omega$$

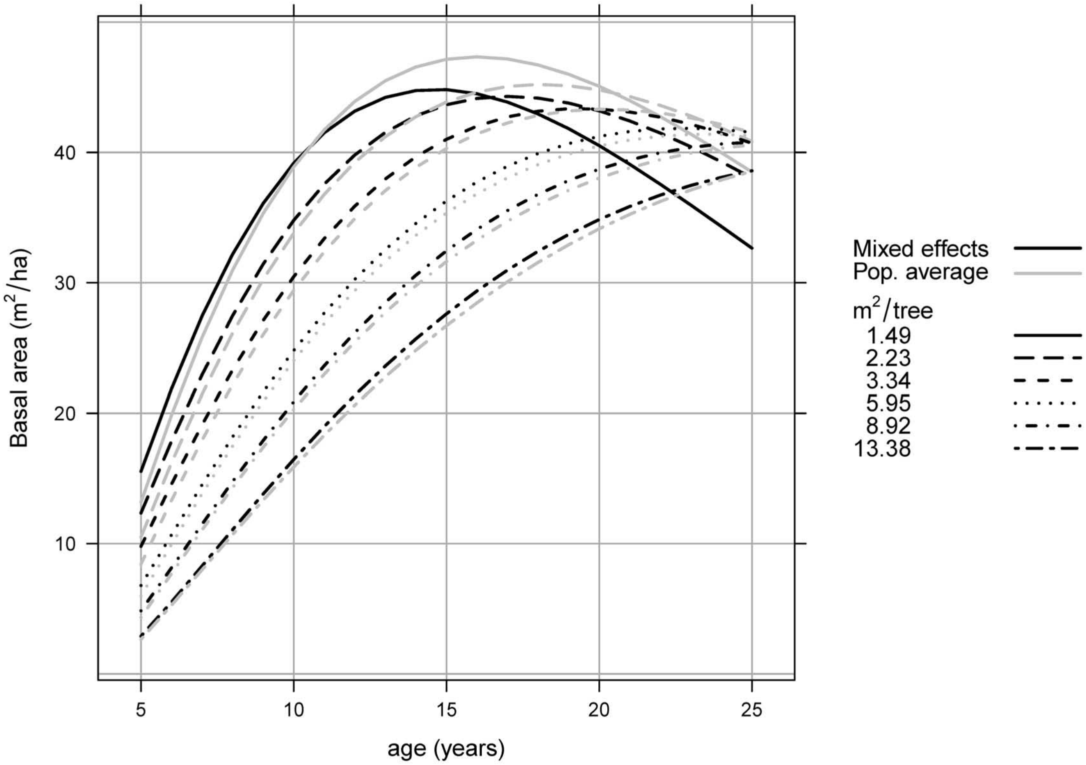


**Figure 6. Predicted BA for the mixed-effects (11) and PA (3) models for six selected initial spacings present in the data set.**

$$b_{2i} \sim N(\mathbf{0}, \boldsymbol{\Psi}_1) \quad \begin{pmatrix} b_{1ij} \\ b_{2ij} \\ b_{3ij} \end{pmatrix} \sim N(0, \boldsymbol{\Psi}_2) \quad \begin{pmatrix} b_{1ijk} \\ b_{3ijk} \end{pmatrix} \sim N(0, \boldsymbol{\Psi}_3)$$

$$i = 1, \ldots, 4; \quad j = 1, \ldots, 3; \quad k = 1, \ldots, 16;$$

$$l, l' = 1, \ldots, 25$$

$$\hat{\boldsymbol{\Psi}}_1 = \hat{\Psi}_1$$

$$\hat{\boldsymbol{\Psi}}_2 = \begin{pmatrix} \hat{\Psi}_{2,11} & 0 & 0 \\ 0 & \hat{\Psi}_{2,22} & 0 \\ 0 & 0 & \hat{\Psi}_{2,33} \end{pmatrix}$$

$$\hat{\boldsymbol{\Psi}}_3 = \begin{pmatrix} \hat{\Psi}_{3,11} & \hat{\Psi}_{3,13} \\ \hat{\Psi}_{3,31} & \hat{\Psi}_{3,33} \end{pmatrix}$$

$$\boldsymbol{\varepsilon}_{ijkl} \sim N(\mathbf{0}, \sigma^2 \boldsymbol{\Lambda}_{ijkl})$$

$$\mathrm{Var}(\varepsilon_{ijkl}) = \sigma^2 |A_{ijkl}|^{2\delta_{1,i}} |S_{ijkl}|^{2\delta_{2,i}}$$

The structure of the within-group error $\varepsilon_{ijkl}$ was modeled with an autoregressive model AR(1) with correlation parameter estimate $\kappa$. The variance was modeled with a combination of two power variance models, one with age as covariate and one with initial spacing as covariate and both with parameters that change by location. The residuals of the final model did not present any discernible pattern by location or spacing. We also explored the possibility of a trend between the random effects and site quality. Because dominant height is affected by initial spacing (Antón-Fernández et al. 2011), we defined site index as the average height of trees with dbh larger than the quadratic mean diameter at age 25 in the widest spacing (13.38 $m^2$/tree), $SI_{13.38}$. We assigned an estimate of $SI_{13.38}$ for each replicate (three per location). When possible, $SI_{13.38}$ was the observed dominant height at age 25; for the rest of the cases where dominant height at age 25 in the widest spacing was not available, $SI_{13.38}$ was estimated using a ME model for dominant height specifically fitted to that data set. When the estimates of the random effects at the replicate level were plotted against $SI_{13.38}$ (Figure 5) no discernible pattern was

**Table 3. Estimates and lower and upper confidence limits of the parameters for the PA approach model 3.**

| | Estimate | Lower | Upper |
|---|---|---|---|
| $\alpha_0$ | 2.98640 | 2.45716 | 3.51564 |
| $\alpha_1$ | −0.09791 | −0.13324 | −0.06258 |
| $\alpha_2$ | 5.79073 | 4.50277 | 7.07868 |
| $\omega_0$ | 2.90716 | 2.71296 | 3.10137 |
| $\omega_1$ | 0.06276 | 0.03607 | 0.08945 |
| $\beta$ | 1.24643 | 1.19196 | 1.30091 |
| $\theta_0$ | −0.06393 | −0.07292 | −0.05494 |
| $\theta_1$ | 0.00189 | 0.00118 | 0.00260 |
| $\theta_2$ | −0.05174 | −0.06994 | −0.03353 |
| $\kappa_1$ | 1.89990 | 1.92374 | 1.86175 |
| $\kappa_2$ | −0.91449 | −0.94296 | −0.87275 |
| $\rho$ | −0.84918 | −0.89941 | −0.77681 |
| $\delta_{1,P1}$ | 0.17029 | 0.23957 | 0.30886 |
| $\delta_{1,P2}$ | 0.17009 | 0.24683 | 0.32357 |
| $\delta_{1,C1}$ | 0.35750 | 0.41426 | 0.47101 |
| $\delta_{1,C2}$ | 0.39927 | 0.45900 | 0.51872 |
| $\delta_{2,P1}$ | −0.60728 | −0.52609 | −0.44489 |
| $\delta_{2,P2}$ | −0.36170 | −0.26738 | −0.17305 |
| $\delta_{2,C1}$ | −0.66945 | −0.59705 | −0.52465 |
| $\delta_{2,C2}$ | −0.66485 | −0.59431 | −0.52376 |

All parameters were statistically significant at $\alpha = 0.001$.

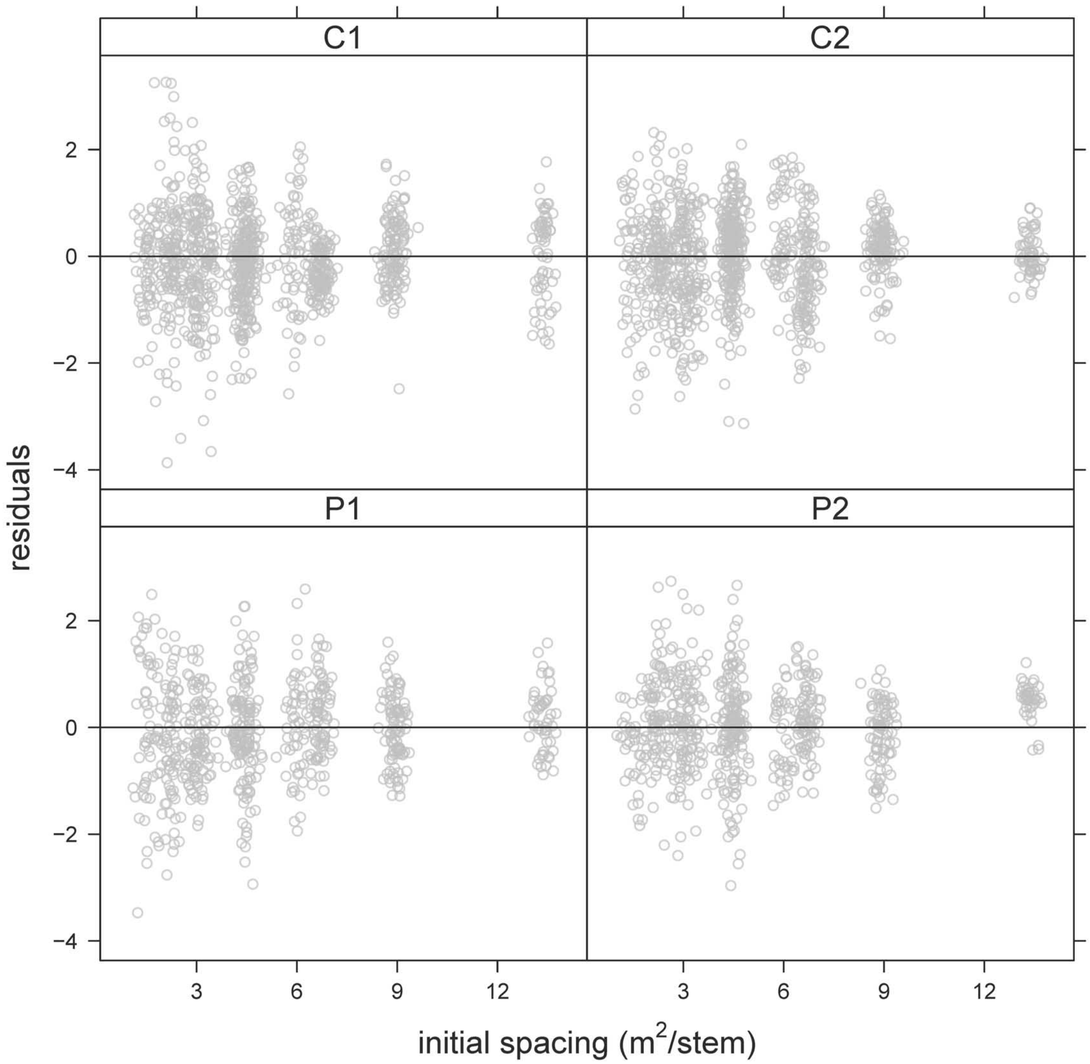


**Figure 7. Within-group residuals for the ME model by location, showing heteroscedasticity of the residuals with respect to initial spacing when only heteroscedasticity along the age covariate is taken into account.**

present for $b_{3ijk}$. The other two estimated random-effects parameters ($b_{2ijk}$ and $b_{1ijk}$) showed a weak tendency to decrease with increasing site index. The range of $SI_{13.38}$ in the data set was approximately 2 m.

Figure 6 shows the patterns of BA development by initial spacing. BA at the closest initial spacing reaches its maximum at approximately age 15 and then starts to decrease, crossing over the curves of the wider initial spacings. As initial spacing increases (density decreases), the maximum BA reached and the rate at which it is reached diminish. Thus, closer initial spacings reach their maximum sooner and approach it faster than wider initial spacings.

## *PA Model*

The final form of the PA model is Equation 3, with structure of the within-group error $\varepsilon_{ijkl}$ modeled with an autoregressive moving average ARMA(2, 1) model with autoregressive parameters ($\kappa_1$, $\kappa_2$) and moving average parameter $\rho$. The variance was modeled, similarly to the ME model, with a combination of two power variance models: one with age as covariate and one with initial spacing as covariate. Both contain parameters that change by location:

$$\mathrm{Var}(\varepsilon_{ijkl}) = \sigma^2 |A_{ijkl}|^{2\delta_{1,i}} |S_{ijkl}|^{2\delta_{2,i}}.$$

The parameter estimates for the final PA model, including lower and upper confidence limits are shown in Table 3. All parameters are significant at $\alpha = 0.001$.

Differences in the behavior of the PA and ME models for the fitting data set were small except for initial spacings less than 3 m$^2$/tree (Figure 6). The PA model at the closest spacings reached a higher maximum carrying capacity, and it did so at an older age than the ME model. For the closest initial spacing, the PA and the ME models start to diverge at approximately age 12. The PA and ME models for the closest initial spacings do not converge at age 25 nor do they show any tendency toward convergence. At age 25, the difference between the PA and ME models for the closest initial spacing is 6 m$^2$/ha.

**Table 4. Log-likelihood and model selection criteria for different modeling options of the within-group error variance.**

| | AIC | BIC |
|---|---|---|
| ME model with $\mathrm{Var}(\varepsilon_{ijkl}) = \sigma^2 \lvert A_{ijk} \rvert^{2\delta_{1,i}}$ | 10,059 | 10,193 |
| ME final model | 9,529 | 9,688 |
| PA model with $\mathrm{Var}(\varepsilon_{ijkl}) = \sigma^2 \lvert A_{ijkl} \rvert^{2\delta_{1,i}}$ | 10,546 | 10,650 |
| PA final model | 9,942 | 10,071 |

AIC, Akaike information criterion; BIC, Bayesian information criterion.

### *Heteroscedasticity and Autocorrelation*

Heteroscedasticity was present in the residuals of both models. The variance of the residuals of the models increased with age and decreased with initial spacing. Even after accounting for heteroscedasticity in the age covariate, there was a pattern in the residuals of the models along the initial spacing covariate (e.g., Figure 7). Accounting for heteroscedasticity in both covariates improved the fit of the models (Table 4).

## Discussion and Conclusion

The two models proposed in this study describe the effect of a wide range of initial spacing on the BA development of loblolly pine stands. The basic form of the models is a modified type II combined exponential and power function, which allows the asymptotic behavior of stand BA for wide initial spacing stands and a decrease in BA after reaching its maximum for close initial spacing. When used for predictions, the PA model is more accurate when no previous measurements are available. If previous measurements are available, the ME model could give more accurate estimates (e.g., Meng et al. 2009).

As initial density increases, the variability of stand BA also increases. The within-group error variance increased with closer initial spacing, as shown by Figure 7 and as indicated by the sign of the within-group error variance parameters in Tables 2 and 3. In addition, in the ME model, the random effects affecting parameters $\alpha$ and $\theta$ were significant in $S^{-1}$, but not in $S$, indicating that differences among blocks and among plots decreased as initial spacing increased. Consequently, under similar conditions, predictions of BA for closer initial spacings would probably be less precise than predictions for wider spacings.

BA development models for loblolly pine often include a measure of site quality, generally site index, as a covariate in the model (e.g., Harrison and Daniels 1988, Hasenauer et al. 1997). However, we found no evidence of an effect of site quality on BA development for the spacing trial data used. There was relatively little variability in $SI_{13.38}$ across the spacing study; thus, the effect of site index on BA development may not be discernible.

If the main interest is on the fixed effects, the ME and PA approaches are generally nearly equivalent (Pinheiro 2006), and, in some cases, it is even possible to derive marginal quantities from a nonlinear ME model (Lee and Nelder 2004, Serroyen et al. 2009). However, even when similar inferences on the fixed effects can usually be obtained from the fixed effects of the ME and PA approaches, there are cases for which both approaches cannot be considered equivalent, such as the models presented here. Because PA models are more accurate than ME models when no previous measurements are available, we recommend the use of the PA model for this situation and the use of the ME model when previous measurements are available.

In conclusion, stand BA development for a wide range of initial planting densities of loblolly pine can be represented with a combined exponential and power function. Both population average and ME modeling methods produced satisfactory results when fitted with data from a 25-year-old spacing trial. Based on information available, an appropriate fitted model can be applied. If previous observations are available, that information can be used with the ME model to improve accuracy of predictions; when no previous observations are available, the PA model is the preferred option.

## Literature Cited


AKAIKE, H. 1974. A new look at the statistical model identification. *IEEE Trans. Autom. Control* 19(6):716–723.

AMATEIS, R.L., AND H.E. BURKHART. 1996. Impact of heavy glaze in a loblolly pine spacing trial. *South. J. Appl. For.* 20(3):151–155.

ANTÓN-FERNÁNDEZ, C., H.E. BURKHART, M. STRUB, AND R.L. AMATEIS. 2011. Effects of initial spacing on height development of loblolly pine. *For. Sci.* 57(3):201–211.

BAILEY, R.L., G.E. GRIDER, J.W. RHENEY, AND L.V. PIENAAR. 1985. *Stand structure and yields for site-prepared loblolly pine plantations in the Piedmont and upper coastal plain of Alabama, Georgia, and South Carolina.* Res. Bull. 328. Univ. of Georgia Exp. Stations. 118 p.

BUFORD, M.A. 1991. Performance of four yield models for predicting stand dynamics of a 30-year-old loblolly pine (*Pinus taeda* L.) spacing study. *For. Ecol. Manag.* 46(1–2):23–38.

BURKHART, H.E., AND P.T. SPRINZ. 1984. Compatible cubic volume and basal area projection equations for thinned old-field loblolly pine plantations. *For. Sci.* 30(1):86–93.

DAVIDIAN, M., AND D.M. GILTINAN. 1995. *Nonlinear models for repeated measurement data.* Chapman & Hall, London, UK.

DIGGLE, P., P. HEAGERTY, K.Y. LIANG, AND S. ZEGER. 2002. *Analysis of longitudinal data.* Oxford University Press, New York.

HARRISON, W.C., AND R.F. DANIELS. 1988. A new biomathematical model for growth and yield of loblolly pine plantations. P. 293–304 in *Forest growth modeling and prediction: Proceedings IUFRO conference* vol. 1, Ek, A.R., S.R. Shifley, and T.E. Burk (eds.). US For. Serv. GTR-NC-120. North Cent. For. Exp. Stn., Minneapolis, MN.

HASENAUER, H., H.E. BURKHART, AND R.L. AMATEIS. 1997. Basal area development in thinned and unthinned loblolly pine plantations. *Can. J. For. Res.* 27(2):265–271.

LEE, Y., AND J.A. NELDER. 2004. Conditional and marginal models: Another view. *Statist. Sci.* 19(2):219–238.

LINDSTROM, M.J., AND D.M. BATES. 1990. Nonlinear mixed effects models for repeated measures data. *Biometrics* 46(3): 673–687.

MATNEY, T.G., AND A.D. SULLIVAN. 1982. Compatible stand and stock tables for thinned and unthinned loblolly pine stands. *For. Sci.* 28(1):161–171.

MENG, S.X., S. HUANG, Y. YANG, G. TRINCADO, AND C.L. VANDERSCHAAF. 2009. Evaluation of population-averaged and subject-specific approaches for modeling the dominant or codominant height of lodgepole pine trees. *Can. J. For. Res.* 39(6):1148–1158.

PINHEIRO, J.C. 2006. Conditional versus marginal covariance representation for linear and nonlinear models. *Aust. J. Statsit.* 35(1):31–44.

PINHEIRO, J.C. AND D.M. BATES. 2000. *Mixed-effects models in S and S-PLUS.* Springer, New York.

PINHEIRO, J., D. BATES, S. DEBROY, D. SARKAR, AND R CORE TEAM. 2009. *nlme: Linear and nonlinear mixed effects models.* R package version 3.1-96.

R DEVELOPMENT CORE TEAM. 2009. *R: A language and environment for statistical computing.* R Foundation for Statistical Computing, Vienna, Austria.

RADTKE, P.J., AND H.E. BURKHART. 1999. Basal area growth and crown closure in a loblolly pine spacing trial. *For. Sci.* 45(1):35–44.

SCHWARZ, G. 1978. Estimating the dimension of a model. *Ann. Statist.* 6(2):461–464.

SERROYEN, J., G. MOLENBERGHS, G. VERBEKE, AND M. DAVIDIAN. 2009. Nonlinear models for longitudinal data. *Am. Statist.* 63(4):378–388.

SHARMA, M., H.E. BURKHART, AND R.L. AMATEIS. 2002a. Modeling the effect of density on the growth of loblolly pine trees. *South. J. Appl. For.* 26(3):124–133.

SHARMA, M., H.E. BURKHART, AND R.L. AMATEIS. 2002b. Spacing rectangularity effect on the growth of loblolly pine plantations. *Can. J. For. Res.* 32(8):1451–1459.

SIT, V. AND M. POULIN-COSTELLO. 1994. *Catalog of curves for curve fitting.* Biometrics Information Handbook, no. 4. Ministry of Forests, Victoria, BC, Canada.

VON GADOW, K., AND G. HUI. 1999. *Modelling forest development.* Kluwer Academic Publishers, Dordrecht, The Netherlands.

ZEGER, S.L., K.Y. LIANG, AND P.S. ALBERT. 1988. Models for longitudinal data: A generalized estimating equation approach. *Biometrics* 44(4):1049–1060.

ZHAO, D., M. WILSON, AND B.E. BORDERS. 2005. Modeling response curves and testing treatment effects in repeated measures experiments: A multilevel nonlinear mixed-effects model approach. *Can. J. For. Res.* 35(1):122–132.